Nanophysics

Brief notes
L. Zampieri

October 11, 2020

Contents

1 Nanothermodynamics **2**
1.1 Melting temperature: Pawlow model . . . 2
1.2 Melting temperature: liquid-layer model . . . 3
1.3 Melting temperature: other models . . . 4

2 Nucleation **4**
2.1 GibbsThompson equation . . . 5
2.2 DLA dynamics . . . 6
2.3 OR dynamics . . . 6
2.4 Growing control . . . 7

3 Ion implantation **8**
3.1 Binary collisions . . . 9
3.2 Interesting quantities . . . 9
3.3 Other effects . . . 10

4 Optical properties **10**
4.1 Quasi-static dipolar approximation . . . 11
4.2 Multipolar case . . . 13
4.3 Dielectric function . . . 14
4.4 Controlling LSPR . . . 16
4.5 Interacting nanoparticles . . . 16
4.6 Discrete dipolar approximation DDA . . . 18
4.7 Non linear responses . . . 18
4.8 Z-scan . . . 18

5 Observing nanoparticles **19**
5.1 X-Ray diffraction . . . 19
5.2 Electron microscopy . . . 20
5.3 Near field optical properties . . . 20

6 Applications **21**
6.1 Biosensing . . . 21
6.2 Self-similar nanolens . . . 22
6.3 Emitters . . . 22

7 Propagation and confinement of photons **23**
7.1 Photonic crystals . . . 24

8 Metamaterials **25**
8.1 Obtain metamaterials 26
8.2 Anisotropic metamaterials 27
8.3 Hyperbolic materials 27

1 Nanothermodynamics

When considering a nanometric system, one must consider that the size of the system itself is comparable to physical quantities which are typically considered much small, such as electrons mean free path, bohr radius and magnetic domains mean radius. This means that the size of the system cannot be assumed *much larger* in computing expectation values.

A first approximation of this phenomena, considering a physical quantity A as function of the total number of entities N or the characteristic length R, is given by the size equation:

$$A(N) = A_\infty \left(1 + \frac{C_N}{N^\alpha}\right) \qquad A(R) = A_\infty \left(1 + \frac{C_R}{R^\alpha}\right)$$

where C_N/C_R and α are typically phenomenologically retrieved. Observe that, since N is an integer and R is lower-bounded by bohr radius, these equations are well defined and there are no divergence problems.

Surface fraction As the size of the system decreases, the fraction of atoms that are in contact with the surface grow up: consider in fact a cluster of N atoms, each with radius R_0:

$$V = \frac{4}{3}\pi N R_0^3 \quad \rightarrow \quad R_{cluster} = \sqrt[3]{N} R_0$$
$$F = \frac{4\pi R_{cluster}^2 / 4\pi R_0^2}{4/3\pi R_{cluster}^3 / 4/3\pi R_0^3} = \frac{4}{\sqrt[3]{N}}$$

i.e., the fraction of surface atoms goes like $N^{-1/3}$, and therefore is not negligible for nanometric particles.

1.1 Melting temperature: Pawlow model

Melting temperature behavior is a typical example of size dependence of physical quantities. Remembering that along the coexistence line:

$$\mu_L(T, P) = \mu_S(T, P)$$

and being T_0, P_0 a known point of coexistence, one can expand:

$$\begin{aligned}\mu_L(T, P) &= \mu_L(T_0, P_0) + \frac{\partial \mu_L}{\partial T} + \frac{\partial \mu_L}{\partial P} + \dots \\ &= \mu_L^0 - s_L(T - T_0) + \frac{1}{\rho_L}(P_L - P_0)\end{aligned}$$

Along the coexistence line, therefore,

$$\mu_L^0 - s_L(T - T_0) + \frac{1}{\rho_L}(P_L - P_0) = \mu_S^0 - s_S(T - T_0) + \frac{1}{\rho_S}(P_S - P_0)$$
$$(s_L - s_S)(T - T_0) - \frac{P_L - P_0}{\rho_L} + \frac{P_S - P_0}{\rho_S} = 0$$

Let's now consider the Laplace equation of a soap bubble pressure, as function of surface tension γ:

$$P_L = P_{ext} + \frac{2\gamma_L}{R_L} \qquad P_S = P_{ext} + \frac{2\gamma_S}{R_S}$$

It result:

$$T_0(s_L - s_S)(\frac{T}{T_0} - 1) + P_0 \left(\frac{1}{\rho_L} - \frac{1}{\rho_S}\right) + \frac{P_S}{\rho_S} - \frac{P_L}{\rho_L} = 0$$
$$T_0(s_L - s_S)(\frac{T}{T_0} - 1) + P_0 \left(\frac{1}{\rho_L} - \frac{1}{\rho_S}\right) + \frac{2\gamma_S}{\rho_S R_S} - \frac{2\gamma_L}{\rho_L R_L} = 0$$

Considering the definition of latent heat $L = T_0(s_L - s_S)$ and the atom number conservation $\rho_S R_S^3 = \rho_L R_L^3$, one can rewrite:

$$\frac{T}{T_0} - 1 = -\frac{2}{LR_S\rho_S}\left[\gamma_S - \gamma_L\left(\frac{\rho_S}{\rho_L}\right)^{2/3}\right]$$

which is exactly in the shape of a size equation,

$$T = T_0\left(1 + \frac{A}{R_S}\right)$$

This approximation correctly predict the trend of the melting temperature, but fails in fitting data at lower radius; higher-order models must be considered.

1.2 Melting temperature: liquid-layer model

Consider a fully liquid particle: $G_L = N\mu_L + 4\pi R_L^2\gamma_{LV}$.
Consider a fully solid particle: $G_S = N\mu_S + 4\pi R_S^2\gamma_{SV}$.
Consider a fully-solid-to-fully-liquid transition:

$$\begin{aligned}\Delta G_{LS} &= N(\mu_L - \mu_S) + 4\pi(R_L^2\gamma_{LV} - R_S^2\gamma_{SV}) \\ &= \frac{4}{3}\pi R_S^3\rho_S L(1 - \frac{T}{T_0}) + 4\pi R_S^2\left[\gamma_{LV}\left(\frac{\rho_S}{\rho_L}\right)^{2/3} - \gamma_{SV}\right]\end{aligned}$$

The transition is when the system reach an equilibrium, i.e. when $\frac{\partial G}{\partial R} = 0$. Solving the latter, one obtain the same result of the Pawlow model. Consider instead the possibility of the formation of a liquid layer which reflect the graduality in cluster melting: let be δ the thickness of this liquid layer, over the R total radius (let's consider the approximation $\rho := \rho_S = \rho_L$ and $R := R_S = R_L$):

$$\begin{aligned}\Delta G &= \left[(N - N_{LL})\mu_S + N_{LL}\mu_L\right] - N\mu_S + \left[4\pi R^2\gamma_{LV} + 4\pi(R-\delta)^2\gamma_{SL}\right] - 4\pi R^2\gamma_{SV} \\ &= N_{LL}(\mu_L - \mu_S) + 4\pi R^2\left[\gamma_{LV} + \left(1 - \frac{\delta}{R}\right)^2\gamma_{SL} - \gamma_{SV}\right]\end{aligned}$$

Solving $\frac{\partial \Delta G}{\partial R} = 0$ one obtain

$$T = T_0\left(1 - \frac{A}{R - \delta}\right)$$

or, relaxing the previous approximation and considering $\rho_L \neq \rho_S$,

$$T = T_0\left(1 - \frac{A}{R-\delta} - \frac{B}{R}\right)$$

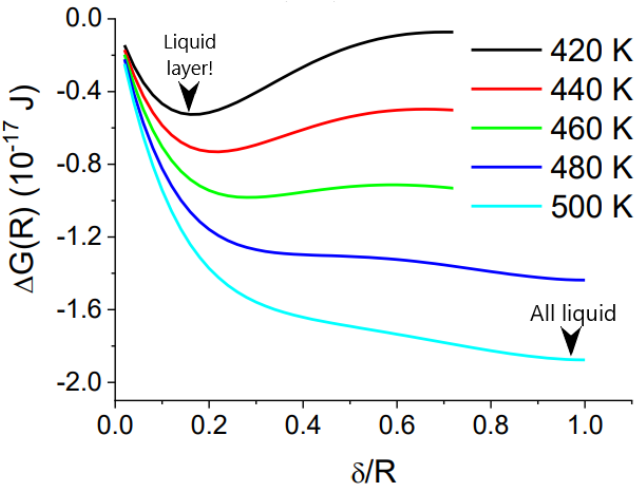

Figure 1: Liquid layer model

The liquid layer can be experimentally observed through electrons microscopy.

1.3 Melting temperature: other models

Other models are available to study melting temperature trend: e.g., considering smooth interface interaction, or a coherence length in surface tension.

Moreover, in some experiments, secondary effects have been observed, as e.g. hysteresis (superheating and supercooling) and a bimodal particle radius distribution. These effect are typically ascribed to the matrix: on one hand, pressure of silica matrix on nanoclusters can affect free expansion; secondly, this pressure heat the particles; finally, an oxide layer can produce: even if nanoparticles are already melted, in the surface between NPs and matrix there can be an oxide layer produced by the interaction between matrix, NPs and atmosphere, that is still solid and confine the liquid as a bubble.

2 Nucleation

Nucleation processes are the ones responsible of atoms aggregation for the formation of NPs. Nucleation can be homogeneous or heterogeneous: in the first case is start from a random atom cluster, while in the second ones the impurities in the system work as catalyst to start the nucleation.

A first, simplified model can be described considering the condensation energy:

$$\Delta G = -N\Delta g_N + 4\pi R^2\gamma$$

where the first term describe the transition between gas and liquid, which stabilize the system, while the second one describe the formation of a surface, which destabilize the system.

Being R the effective radius $R = \sqrt[3]{N}R_0$, δg_N the variation of free energy per particle $\delta g_N = \delta\mu_{LV} = k_B T \ln P^*$, P^* the pressure normalized to the vapour pressure $P^* = P/P_e$. Performing this substitutions:

$$\Delta G = -Nk_B T \ln P^* + 4\pi\gamma R_0^2 \sqrt[3]{N}$$

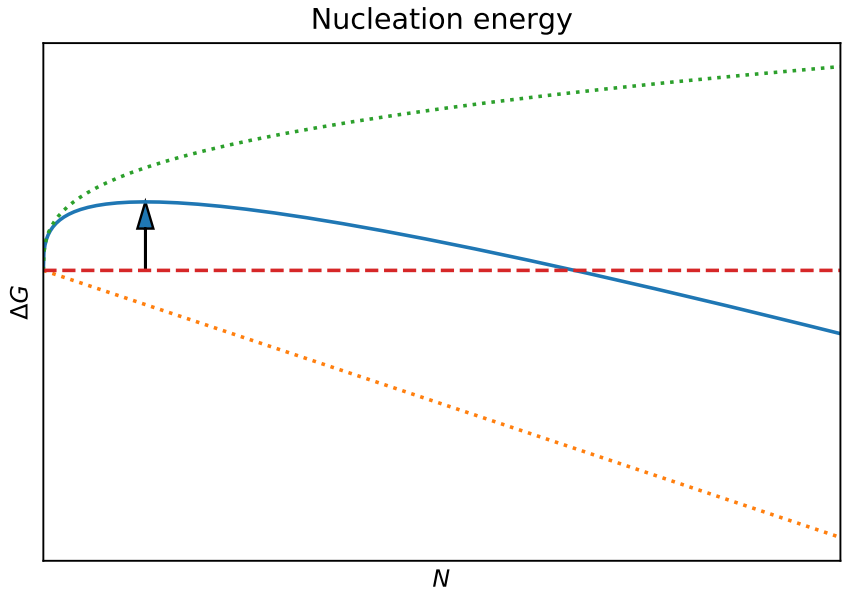

Figure 2: Nucleation energy, with energy barrier highlighted

The energy barrier that a vapour system must overcome to reach the left side of the plot, i.e. the spontaneous growing state, can be computed nullifying the ΔG derivative:

$$\Delta G^* = \frac{16\pi\gamma^3}{3\rho k_B T \ln P^*}$$

which lead to the nucleation speeed $J \propto e^{-\beta\Delta G^*}$

2.1 GibbsThompson equation

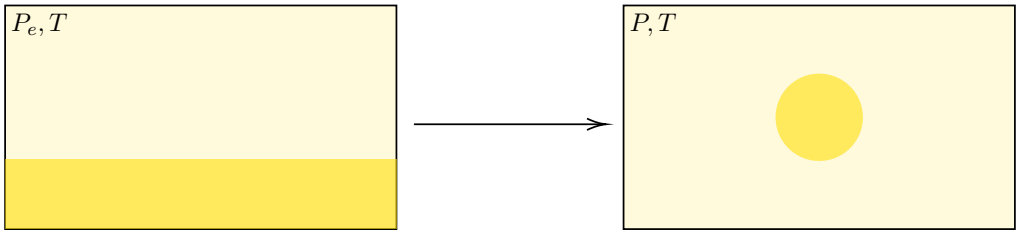

Figure 3: Formation of a nanoparticle

A more complete model can be built considering a transition between a bulk liquid-vapour equilibrium to a nanoliquid-vapour one: observe that the system is in a pressure equilibrium in both cases! The transition can be split in 3 steps.

Vapour from P_e to P

$$\Delta G_1 = N k_B T \ln \frac{P}{P_e} \quad \rightarrow \quad \mu_V[P] = \mu_V[P_e] + k_B T \ln \frac{P}{P_e}$$

Liquid bulk from P_e to P Since liquid is incompressible, $\Delta G_2 = 0$.

Liquid from bulk to nanosphere Since the system is in equilibrium in both sides,

$$\mu_L^R[P] = \mu_V[P] \qquad \mu_L^\infty[P_e] = \mu_V[P_e]$$

But, from the usual surface tension equation,

$$\mu_L^R[P] = \mu_L^\infty[P] + \frac{2\gamma}{\rho R}$$

Combining the results of the three points:

$$\begin{aligned} \mu_L^R[P] &= \mu_L^\infty[P] + \frac{2\gamma}{\rho R} \\ \mu_V[P] &= \mu_L^\infty[P_e] + \frac{2\gamma}{\rho R} \\ \mu_V[P_e] + k_B T \ln \frac{P}{P_e} &= \mu_L^\infty[P_e] + \frac{2\gamma}{\rho R} \end{aligned}$$

which lead to

$$P(R) = P_e \exp\left\{\frac{2\gamma}{k_B T \rho R}\right\}$$

where $P(R)$ is the vapour equilibrium pressure for nanoparticles of radius R. The latter is called *Gibbs Thompson equation*: it shows that the pressure increase as the nanoparticles radius decrease. This lead to the formation of two possible scenarios:

Diffusion Limited Aggregation DLA If P is greater than $P(R)$ for all the nanoparticles, they all grow; the growing is limited only by diffusion speed;

Ostwald Ripening OR If P is greater than $P(R)$ for largest particles, but lower for smallest ones, there is a competitive growth: smallest particles dissolve in a under-saturated environment, while largest ones grow even more.

2.2 DLA dynamics

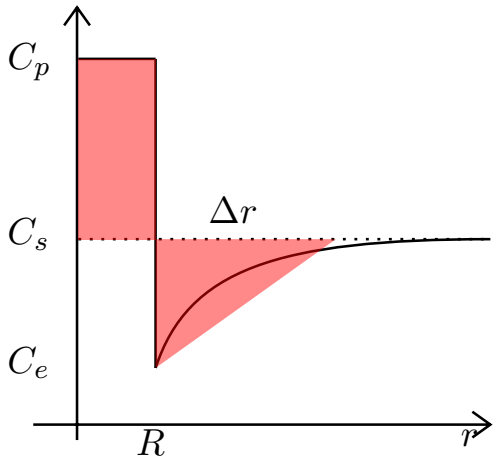

Figure 4: Concentration

In DLA-controlled dynamics, the concentration profile can be modelled as in fig. 4. Consider the particle boundary: the growth in size of the particle must be equal to the number of particles that reach the boundary via diffusion. In equation,

$$4\pi R^2(C_p - C_e)\frac{\mathrm{d}R}{\mathrm{d}t} = 4\pi R^2 D\frac{\partial C}{\partial r}\bigg|_{R^+}$$

where C_p is the concentration inside the NP, while C_e is the concentration just outside the boundary. Let's approximate the concentration outside with a linear dumping: for the conservation of matter,

$$(C_p - C_s)R = \frac{1}{2}(C_s - C_e)\Delta r$$
$$\Delta r = 2\frac{C_p - C_s}{C_s - C_e}R$$
$$C = C_e + \frac{C_s - C_e}{\Delta r}(r - R)$$
$$\frac{\partial C}{\partial r}\bigg|_{R^+} = \frac{C_s - C_e}{\Delta r} = \frac{(C_s - C_e)^2}{2(C_p - C_s)R}$$

and, substituting in the previous equation,

$$(C_p - C_e)\frac{\mathrm{d}R}{\mathrm{d}t} = D\frac{(C_s - C_e)^2}{2(C_p - C_s)R}$$
$$R^2 = R_0^2 + D\frac{(C_s - C_e)^2}{(C_p - C_s)(C_p - C_e)}t$$
$$\boxed{R^2 = R_0^2 + \kappa_1 t}$$

where the last equation describes the growth dynamics in DLA!

2.3 OR dynamics

Disclaimer This paragraph is wrong. I'm sorry, I'm still not able to came out from this stuff.

In the Ostwald Ripening regime, the growth dynamics is a bit different. Consider in fact GibbsThompson equation:

$$P = P_\infty \exp\left\{\frac{2\gamma}{k_B T \rho R}\right\}$$

which means, expanding to the first order for large R and remembering $P \propto C$:

$$C(R) = C_\infty \left(1 + \frac{\alpha}{R}\right)$$

where $C(R)$ is the equilibrium concentration at radius R. In a first approximation, one can consider the nanoparticle always in equilibrium with the enviroment. the external concentration C_e can be considered as not dependent from the diffusion, but always in equilibrium with the nanoparticle: $C_e(r) = C(R)$. Therefore:

$$\left.\frac{\partial C}{\partial r}\right|_{R^+} = \left.\frac{\partial}{\partial r} C_\infty \left(1 + \frac{\alpha}{R}\right)\right|_{R^+} = -\frac{C_\infty \alpha}{R^2}$$

Recalling the equation from DLA growing:

$$4\pi R^2 (C_p - C_e)\frac{\mathrm{d}R}{\mathrm{d}t} = 4\pi R^2 D \left.\frac{\partial C}{\partial r}\right|_{R^+}$$
$$(C_e - C_p)\frac{\mathrm{d}R}{\mathrm{d}t} = D\frac{C_\infty \alpha}{R^2}$$

where it has been considered that typically $C(R) > C_p$.Solving the last differential equation:

$$R^3 = R_0^3 + \kappa_2 t$$

Sounds false. Vapour pressure greater than bulk pressure? Impossible. But otherwise signs aren't compatible...

which describes the growth dynamics in OR!

These results clearly show that there are two regimes in the growing, with two different trends.

2.4 Growing control

The growing process can be controlled through different parameters. For example, the temperature: when the sample is loaded with a supersaturated concentration of metal, it must be annealed for some time while nanoparticles grow up. A plot of the mean radius as function of the temperature (at fixed annealing time) is reported in fig. 5.

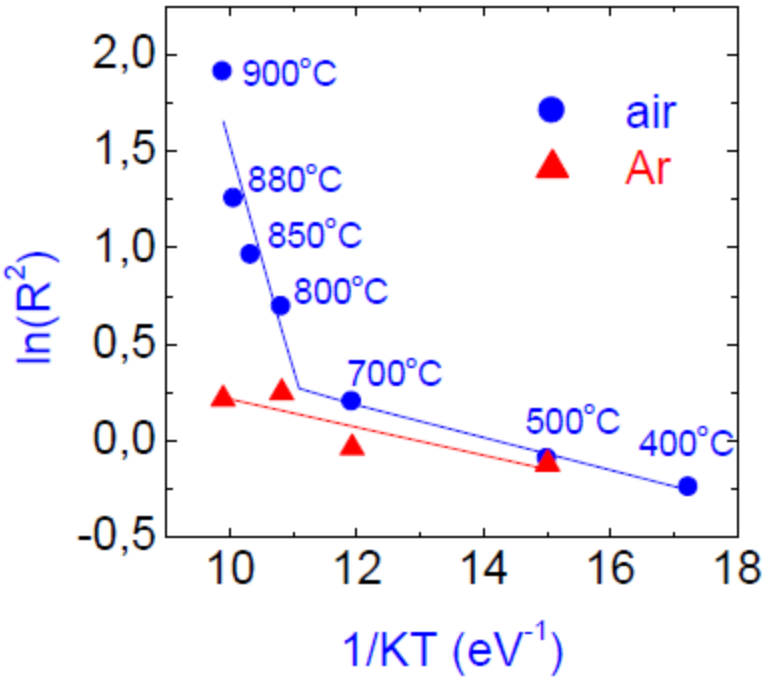

Figure 5: Mean radius of gold nanoparticles after 1h annealing, as function of annealing time and atmosphere, in a silica matrix.

As can be seen from the plot, the temperature can be used to control the nanoparticles radius, as higher temperatures correspond to larger radius. On the other hand, a particular knee can be seen in the curve of air annealing: this is due to the presence of oxygen. While at lower T the permeability of silica to oxygen is negligible, as the temperature grow up the oxygen starts to permeate the silica matrix, interacting with the diffusion of gold atoms; therefore, correlated two-species diffusion equations must be considered, and the diffusion constant D in DLA and OR dynamics equation must keep in consideration the presence of multiple species diffusing. The atmosphere, therefore, together with the temperature, can be used to control particle growing.

Moreover, also the annealing time is a important way to control the nanoparticles size. It's clear that the more the time pass, the more the nanoparticles radius grow up; typically, a single nanoparticles goes firstly through DLA and then switch to OR. It's oblivious that this transition is not sharp; DLA and OR regime can coexists in systems, contributing both to nanoparticles growth. This is due to the initially distribution of radius, that is clearly not a delta, and can lead to bimodal distributions.

3 Ion implantation

Ion implantation is a technique based on a keV-GeV ion beam hitting the matrix. The absorption process is based on binary collisions, and virtually can be carried out with any element, without saturation constraints: it's easy to obtain supersaturated solutions. Properly setting the beam properties and components, different patterns can be obtained and alloys can be created.

There are lots of different purpose of ion implantation: e.g., the formation of cluster of implanted species, the creation of nucleation spots to induce clusterization of matrix impurities, or the mixing of multilayer matrices.

3.1 Binary collisions

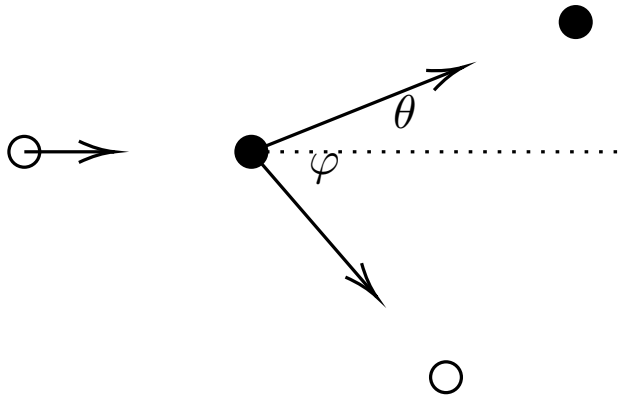

Figure 6: Binary collision

Consider a binary collision, in with an implanted ion (light in the figure 6) hit a matrix atom (dark in the figure): the transferred energy is function of the scattering angle

$$T = \frac{4M_1M_2}{(M_1+M_2)^2}E_0 \sin^2\frac{\theta_C}{2} \qquad \text{with} \quad \theta_C = \theta + \arcsin\left(\frac{M_1}{M_2}\sin\theta\right)$$

If both the bullet and the obstacle are charged, interaction is mediated by coulomb potential

$$V(x) = k\frac{z_1 z_2}{r}e^2\chi(r)$$

where $\chi(r)$ is the screening function due to the fact that the collision happen in a medium.

The transferred energy is typically larger than the atom binding energy, and can lead to ionization or imperfections in the matrices: e.g., displacements, vacancies, interstitial atoms or replacements.

3.2 Interesting quantities

The energy lost in the collision can be split in two contributes: the one given by nuclei, and the other given by electrons.

$$\frac{\mathrm{d}E}{\mathrm{d}x} = \frac{\mathrm{d}E}{\mathrm{d}x}\bigg|_{\text{nuclei}} + \frac{\mathrm{d}E}{\mathrm{d}x}\bigg|_{\text{elec}} = NS(E)$$

where S is the *stopping power*.

The *range* is the average length of the path travelled by the implanted ion inside the matrix:

$$R = \int_{E_0}^{0}\left(\frac{\mathrm{d}E}{\mathrm{d}x}\right)^{-1}\mathrm{d}E = \frac{1}{N}\int_{E_0}^{0}\frac{\mathrm{d}E}{S(E)} \sim \text{nm}$$

while the projected range R_P is the projection of the range on the axis beam. Observe each collision can produce an avalanche effect, so the damaged area can expand way broadener than the implanted ion range, until $3R_P$.

After an implantation, the concentration profile is typically a gaussian, centered on R_P. The dose (also fluence) represent the total quantity of implanted ions per unit of area:

$$C(z) = A\exp\left\{-\frac{1}{2}\left(\frac{z-R_P}{R_P}\right)^2\right\}$$

$$D = \int C(z)\,\mathrm{d}z$$

The total stopping power has two components: the one due to nuclei and the one due to electrons. Their ratio strongly depend on system properties; typically, for light ions $S_e \gg S_n$ while for heavier ones $S_e \sim S_n$.

The process scales governed by tree energies: the displacement energy ($\sim$ 10eV), the lattice binding energy ($\sim$eV, produces vacancies) and the surface binding energy (regulate sputtering). In particular, if there is non-negligible surface sputtering, the concentration profile can be affected by the advancement of the system surface, resulting in a summation of shifted guassians.

3.3 Other effects

The process can interact with already-formed nanoparticles, breaking the surfaces and creating nanoplanets (a big nanoparticles surrounded by lot of smallest satellites nanoparticles).

Sequentially implanting different species, one can fall in different scenarios, depending on substances, matrix, temperature, dose, intensity, order, ...:

- Formation of separated clusters;
- Formation of an alloy;
- Formation of a core-shell geometries...

Phase diagram properties of alloys can be used to control cluster formation; there can exists structural ordered but chemical disordered phases, as well as structural and chemical ordered ones: controlling implantation parameters, the chosen phase can be obtained. Finally, particular temperature and composition combinations can lead elements to non-miscibility phases, leading to alloys decomposition.

Remember that nanoscale properties are not always equals to bulk ones! In nanoscale, for example, is possible the stabilization of bulk metastable states.

To summarize, there are multiple ways to control NP formation with ion implantation, e.g.:

- Control overlapping of concentrations, with dose and energy;
- Chose suitable ions;
- Chose suitable temperature;
- Chose suitable matrix and atmosphere;
- Use radiation.

4 Optical properties

When a radiation cross a system where nanoparticles are present, the absorbance can give information about the crossed medium. The involved quantities are:

- The beam intensity, $I(z,\lambda) = I(0,\lambda)T(z,\lambda)$;
- The transmittance, $T(z,\lambda) = e^{-\gamma(\lambda)z}$;
- The absorbance, $A(z,\lambda) = -\log_{10} T(z,\lambda) = \gamma(\lambda)z$.

The absorption function has been solved by Mie in 1908 in the spherical nanoparticle approximation. Consider a nanoparticle made of an absorbing substance, i.e. with a non-real dielectric function $\varepsilon(\lambda) = \varepsilon_1(\lambda) + \mathrm{i}\varepsilon_2(\lambda)$, in a non-absorbing matrix with a real dielectric function ε_m. In a first approximation, the wave interact with the nanoparticle inducing an oscillation of the electric cloud with a displacement $x(t)$ with respect to the equilibrum position, i.e. inducing a dipole per atom:

$$p = -Nex(t)$$

Let's consider a plane wave $\vec{E} = \vec{E}_0 e^{\mathrm{i}(kz-\omega t)}$: being α the polarizability, the induced polarization is:

$$P = \varepsilon_0 \varepsilon_m \alpha \vec{E}$$

This lead to a separation of the incident field, in transmitted and scattered component:

$$\begin{cases} E_{outside} = E_i + E_s \\ E_{inside} = E_t \end{cases}$$

The system can be considered in two different regimes, depending on the ratio between nanoparticle typical size R and wavelength λ:

- Quasi-static regime: $R \ll \lambda$. The particle feels a uniform field, and a dipolar approximation can be considered;
- Dinamic regime: $R \sim \lambda$. The spatial variations of electric field are not negligible with respect to the particle size, leading to more complex situations and multipolar modes.

4.1 Quasi-static dipolar approximation

Let's start considering a particle subject to a static field, $\vec{E} = E_0\hat{z}$. To respect the system symmetries, the potential can be expanded in radial powers and Legendre polynomials.

$$\psi(r,\theta) = \sum \left[k_l r^l + h_l r^{-(l+1)}\right] P_l(\cos\theta)$$

where θ is the zenith angle with respect to the $\hat{z}$ axis. Clearly, no dependence from the azimuth can appear, otherwise the system symmetry is broken.

Therefore, the potential inside and outside the nanoparticle can be written (observing that inside the particle, to prevent divergence, $h_l = 0\,\forall l$):

$$\begin{cases} \phi_{in}(r,\theta) = \sum A_l r^l P_l(\cos\theta) \\ \phi_{out}(r,\theta) = \sum \left[B_l r^l + C_l r^{-(l+1)}\right] P_l(\cos\theta) \end{cases}$$

The boundary conditions are given by:

- Uniformity at large distances: $\psi_{out} \overset{r\to\infty}{\longrightarrow} -E_0 z$
- Continuity of parallel electric field at particle surface:

$$-\frac{1}{R}\frac{\partial}{\partial\theta}\psi_{in}\Big|_R = -\frac{1}{R}\frac{\partial}{\partial\theta}\psi_{out}\Big|_R$$

- Continuity of perpendicular electric displacement field at particle surface:

$$-\varepsilon_0\varepsilon\frac{\partial}{\partial r}\psi_{in}\Big|_R = -\varepsilon_0\varepsilon_m\frac{\partial}{\partial r}\psi_{out}\Big|_R$$

From these conditions, is not hard to find that:

$$B_l = 0\,\forall l \neq 1 \qquad B_1 = -E_0$$
$$A_l = 0\,\forall l \neq 1$$
$$C_l = 0\,\forall l \neq 1$$

$$\begin{cases} \psi_{in} = -\frac{3\varepsilon_m}{\varepsilon+2\varepsilon_m} E_0 r\cos\theta \\ \psi_{out} = -E_0 r\cos\theta + \frac{\varepsilon-\varepsilon_m}{\varepsilon+2\varepsilon_m} E_0 \frac{R^3}{r^2}\cos\theta \end{cases}$$

where the second term of ψ_{out} can be seen as a dipole field:

$$\psi_{out} = -E_0 r\cos\theta + \frac{1}{4\pi\varepsilon_0\varepsilon_m}\frac{\vec{p}\cdot\vec{r}}{r^3}$$

$$\vec{p} = \underbrace{4\pi R^3 \frac{\varepsilon-\varepsilon_m}{\varepsilon+2\varepsilon_m}}_{\alpha} \varepsilon_0\varepsilon_m\vec{E}_0$$

where the polarizability has been highlighted. Observe that, confirming potential continuity, $\psi_{in}(R) = \psi_{out}(R)$. Finally, this lead to an expression for the electric field:

$$\begin{cases} \vec{E}_{in} = \overbrace{\frac{3\varepsilon_m}{\varepsilon + 2\varepsilon_m}}^{f_e} \vec{E}_0 \\ \vec{E}_{out} = \vec{E}_0 + \frac{1}{4\pi\varepsilon_0\varepsilon_m} \frac{3\hat{r}(\vec{p}\cdot\hat{r}) - \vec{p}}{r^3} \end{cases}$$

where f_e is the field amplification, and it is a complex quantity:

$$f_e = \frac{3\varepsilon_m}{\varepsilon + 2\varepsilon_m} = \frac{3\varepsilon_m(\varepsilon + 2\varepsilon_m)}{(\varepsilon_1 + 2\varepsilon_m)^2 + \varepsilon_2^2}$$

As is clear from the last equation, the field amplification have a resonance when:

$$\varepsilon_1 + 2\varepsilon_m = 0$$

The latter is called *Frölich condition*; moreover, all the previous considerations remains valid if an time oscillation is inserted. Inside the particle, therefore, the electric field is strongly enhanced, and can reach huge values.

Observe that, typically, $\varepsilon_m > 0$: this means that ε_1 must be negative. This is true mainly in metals; therefore, metals are the most used materials for nanoparticle fabrications.

A similar phenomena can be observed in far-field properties; consider complex electric and magnetic fields $\vec{E}_c$ and $\vec{H}_c$, one can write the Poynting vector:

$$\begin{aligned} \vec{S} &= \frac{1}{2}\Re(\vec{E}_c \times \vec{H}_c) \\ &= \frac{1}{2}\Re(\vec{E}_i \times \vec{H}_i + \vec{E}_i \times \vec{H}_s + \vec{E}_s \times \vec{H}_i + \vec{E}_s \times \vec{H}_s) \\ &= \vec{S}_i + \vec{S}_s + \vec{S}_{ext} \end{aligned}$$

where the components from incident field, from scattered field and the mixed one have been highlighted.

The energy flux entering the nanoparticle, i.e. the absorbed energy, is:

$$\begin{aligned} W_a &= -\int_\Sigma \vec{S} \times \mathrm{d}\sigma \\ &= W_i - W_s + W_{ext} \end{aligned}$$

where W_i must be zero by symmetry; the extincted power can be therefore written as:

$$W_{ext} = W_a + W_s$$

or, in terms of cross sections, $\sigma_{ext} = \sigma_a + \sigma_s$; moreover, in terms of efficiencies, $Q_{ext} = Q_a + Q_S$; and finally, in terms of absorption coefficients, $\gamma = \gamma_a + \gamma_s = \rho(\sigma_a + \sigma_s)$.

Dielectric function meaning

Consider the electric susceptibility as a complex quantity:

$$\chi = \chi_1 + \mathrm{i}\chi_2$$

which results in a complex electric permittivity $\varepsilon = 1 + \chi$, and therefore a complex wavevector:

$$\begin{aligned} k &= \omega\sqrt{\varepsilon\varepsilon_0\mu_0} = \frac{\omega}{c}\sqrt{1 + \chi_1 + \mathrm{i}\chi_2} \\ &= \beta + \mathrm{i}\frac{1}{2}\alpha \end{aligned}$$

where β and α has been properly defined to match the previous equation. Consider therefore a plane wave:

$$\begin{aligned} u &= Ae^{\mathrm{i}(kx-\omega t)} = Ae^{\mathrm{i}(\beta x+\mathrm{i}1/2\alpha x-\omega t)} \\ &= Ae^{-1/2\alpha x}e^{\mathrm{i}(\beta x-\omega t)} \end{aligned}$$

where the last exponential is the typical plane wave component, while the first exponential results in a dumping of the amplitude, i.e. an absorption of the wave. Remembering that $I \propto |u|^2 \propto \exp\{-\alpha x\}$, therefore α is the absorption coefficient. Note that there is an ambiguity on the sign of α, due to the double result for a square root; the sign of α is properly chosen such that, if $\chi_2 < 0$, i.e. the medium is absorbing, then $\alpha > 0$, i.e. the wave is attenuating.

Observe that β is nothing but the refractive index n times the vacuum wavevector. Therefore,

$$\varepsilon = \left(n + \mathrm{i}\frac{1}{2}\frac{\alpha}{k_0}\right)^2$$

$$\Re(\varepsilon) = n^2 - \frac{\alpha^2}{4k_0^2}$$

$$\Im(\varepsilon) = \frac{n\alpha}{k_0}$$

The sign of $\Re(\varepsilon)$, therefore, suggests whether the medium is more absorbent of more refractive.

4.2 Multipolar case

If the quasi static approximation is not valid, i.e. the particle radius is comparable with the wavelength, one must consider more complex expansions of the fields: let's again consider complex fields E_c and H_c:

$$\begin{cases} \vec{\nabla} \cdot \varepsilon E_c = 0 \\ \vec{\nabla} \times E_C = i\omega\mu H_c \\ \vec{\nabla} \cdot \mu H_c = 0 \\ \vec{\nabla} \times H_C = -i\omega\varepsilon E_c \end{cases} \longrightarrow \begin{cases} \nabla^2 E_c + k^2 E_c = 0 \\ \nabla^2 H_c + k^2 H_c = 0 \end{cases}$$

with $k^2 = \omega^2\varepsilon\mu$, which means that the electromagnetic wave travel at light speed only in vacuum, while it is slowered in mediums.

The idea is to consider a scalar function, Ψ, and two vectorial functions such that:

$$\begin{cases} M = \vec{\nabla} \times (r\Psi) \\ N = \frac{\vec{\nabla} \times M}{k} \end{cases} \qquad (\nabla^2 + k^2)\Psi = 0$$

Can be easily problem that the last relation is equivalent to $(\nabla^2 + k^2)M = 0, (\nabla^2 + k^2)N = 0$. As before, to respect symmetries, Ψ can be expanded in Spherical Bessel functions and Legendre polynomials, for odd or even Ψ:

$$\Psi^o_{l,m} = j_l(kr)\sin(m\phi)P^m_l(\cos\theta) \tag{1}$$

$$\Psi^e_{l,m} = j_l(kr)\cos(m\phi)P^m_l(\cos\theta) \tag{2}$$

To be precise, j_l are not the Bessel functions, but the Hankel ones, which are complex. The electric fields can be therefore written as:

$$\begin{cases} E_i = E_0 e^{-i\omega t}\sum \mathrm{i}^l \frac{2l+1}{l(l+1)}(M^o_{l1} - \mathrm{i}N^e_{l1}) \\ E_s = E_0 e^{-i\omega t}\sum \mathrm{i}^l \frac{2l+1}{l(l+1)}(\mathrm{i}a_l N^e_{l1} - b_k M^o_{l1}) \\ E_t = E_0 e^{-i\omega t}\sum \mathrm{i}^l \frac{2l+1}{l(l+1)}(c_l M^o_{li} - \mathrm{i}d_l N^e_{l1}) \end{cases}$$

where all the remaining parameters can be computed in terms of the system properties, i.e. μ_m,ε,ε_m and the size parameter kR.

These last equation allow us to compute the electric field in multipolar expansion, as much orders as we want. From these expression, the cross sections can be computed:

$$\sigma_{sca} = \frac{k^4}{6\pi}|\alpha|^2 \propto R^6$$

$$hlc\sigma_{abs} = k\,\Im(\alpha) \propto\sim R^3$$

An explicit expression for the extinction cross section can be obtained considering again the quasi-static approximation $R \ll l$:

$$\sigma_{ext} = 9\frac{\omega}{c}\varepsilon_m^{3/2}V\frac{\varepsilon_2}{(\varepsilon_1+2\varepsilon_m)^2+\varepsilon_2^2}$$

As can be seen, the resonance condition is the same found before, the Frölich condition $\varepsilon_1+2\varepsilon_m = 0$. Some important effects of this formula are:

- The enhancement of the local field;
- The Rayleight scattering: if ε is weakly dependend from λ, can be proven that $\sigma_{sca} \sim \omega^4$, i.e. highest frequencies are strongest scattered;
- Polarization effects: different polarization can correspond to different scattering amplitudes;
- Multipoles: at highest frequencies, i.e. where quasi-static approximation is no more valid, highest polar expansion orders becomes non-negligible. The highest order, opposed to the dipolar one, are more localized to the particle surface: this means that the field enhancement is mainly on the surface. From this, the localized surface plasmonic resonance.
  - Resonance, because is a resonance of the absorbance;
  - Plasmonic, because is given by electrons collective motion;
  - Surface, because its origin is on the presence of a surface splitting two different dielectric function;
  - Localized, because it's strongly localized on nanoparticles.

4.3 Dielectric function

4.3.1 Drude model

Drude model is an approximated model to compute the dielectric function of a metal; it approximate the electrons as classical, free and non interacting.

Let $E = E_0e^{-i\omega t}$ be the external electric field: the motion of electrons can be described as:

$$m\ddot{r} + m\Gamma\dot{r} + \cancel{\tilde{k}r} = -eE_0e^{-i\omega t}$$

where can be recognized the viscosity term due to collisions and the elastic term, that we will neglect. The solution to the differential equation is:

$$r(t) = \frac{eE_0}{m}\frac{\omega^2 - i\omega\Gamma}{\omega^4+(\omega\Gamma)^2}e^{-i\omega t}$$

In fact, let's search for a solution in the form

$$r(t) = \frac{eE}{m}Ae^{-\mathrm{i}\omega t}$$

Replacing in the previous:

$$-eEa\omega^2 - eE\mathrm{i}\omega\Gamma A = -eE$$

$$A = \frac{1}{\omega^2+\mathrm{i}\omega\Lambda} = \frac{\omega^2-\mathrm{i}\omega\Lambda}{\omega^4+(\omega\Lambda)^2}$$

The motions of all the electrons of the metal will produce a dipole:

$$P = -enr(t) \qquad \rightarrow \qquad \chi = \frac{P}{\varepsilon_0 E}$$

$$\varepsilon = 1 + \chi = \underbrace{1 - \frac{\omega_p^2}{\omega^2 + \Gamma^2}}_{\varepsilon_1} + \mathrm{i} \underbrace{\frac{\omega_p^2 \Gamma}{\omega(\omega^2 + \Gamma^2)}}_{\varepsilon_2}$$

$$\omega_p = \sqrt{\frac{ne^2}{m\varepsilon_0}}$$

which allow to compute the dielectric function from the plasma frequency and the scattering one. In the high-frequencies limit, if $\omega \gg \omega_p$, the dielectric function is:

$$\varepsilon = 1 - \frac{\omega_p^2}{\omega^2}$$

i.e., is almost purely real and almost 1. This means that the wavevector is:

$$k = \omega\sqrt{\varepsilon\varepsilon_0\mu\mu_0} = \frac{\omega}{c}\sqrt{1 - \frac{\omega_p^2}{\omega^2}}$$

$$\omega^2 = (kc)^2 + \omega_p^2$$

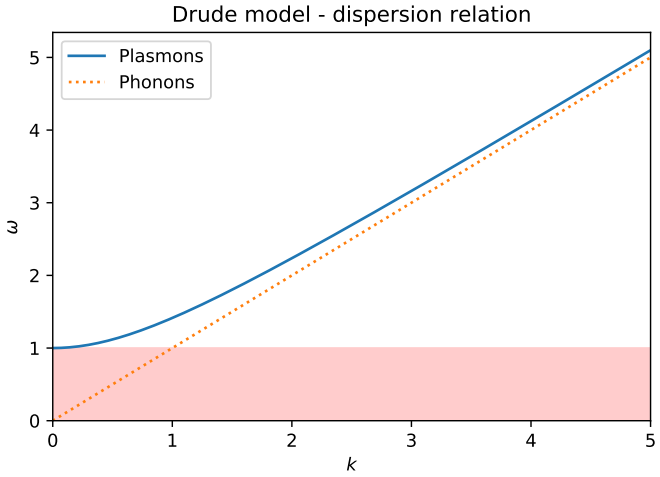

Figure 7: Dispersion relation in drude model. Note that for ω in the red band there are no propagating solutions. Moreover, observe that there is no intersection between the phonon line and the plasmonic one: therefore, a direct conversion from plasmon to phonon is impossible!

Remembering the Frölich condition, one can write:

$$\varepsilon = -2\varepsilon_m = 1 - \frac{\omega_p^2}{\omega^2} \qquad \rightarrow \qquad \omega_{SPR} = \frac{\omega_p}{\sqrt{1 + 2\varepsilon_m}}$$

In real cases, however, other effects must be considered; for example, non conduction-band electrons or interband transitions can affect the dielectric function.

4.3.2 Drude-Lorentz model

The Drude-Lorentz model provide a correction of the Drude model results which consider also bounded electrons:

$$m\ddot{r} + m\Gamma\dot{r} + \tilde{k}r = -eE_0 e^{-i\omega t}$$

Being $\tilde{k} = m\omega_0^2$ and following the same steps of Drude model, one obtain:

$$r(t) = \frac{eE_0}{m}\frac{1}{\omega^2 - \omega_0^2 + i\omega\Gamma}e^{-i\omega t}$$

$$\varepsilon = 1 - \frac{\omega_p^2}{\omega^2 + \mathrm{i}\omega\Gamma} - \sum_j \frac{\omega_{Pj}^2 f_j}{\omega^2 - \omega_{0,j}^2 + i\omega\Gamma_j}$$

with ω_{Pj} the plasma effective frequency for bounded electrons

4.3.3 Size dependence

Consider a small particle: the scattering frequency Γ is given by the bulk electron-electron scattering frequency plus the surface scattering: the average time between two contacts with the surface, given the radius R of the nanoparticle, can be written as

$$\langle\tau\rangle = \frac{4}{\pi}\frac{R}{v_F}$$

which result in a size-dependence of the scattering frequency:

$$\Gamma = \Gamma_{bulk} + \frac{\pi}{4}\frac{v_F}{R}$$

Therefore, the dielectric function can be corrected considering this size dependence. Typically, to obtain the dielectric function for small nanoparticles given the (measured) bulk one ε_∞, the common used relation is:

$$\varepsilon(R) = \varepsilon_\infty - \varepsilon_{drude}(\infty) + \varepsilon_{drude}(R)$$

4.4 Controlling LSPR

There are different ways to control the amplitude and the position of the LSPR:

- Concentration of nanoparticles;
- Nanoparticle materials: using alloys, resonances can be almost freely tuned;
- Size: smallest radius correspond to smallest peaks, highest radius correspond to the appearence of multipolar effects. There is, therefore, an optimal R which correspond to the highest peak;
- Size distribution: if multiple sizes are present,

  $$\chi(\omega) = n\int_0^\infty \sigma_{ext}(\omega, R)f(R)\,\mathrm{d}R$$

  which typically result not in a movement of the peak but in an amplitude variation; therefore, it's usually impossible to obtain $f(R)$ from the peak analysis;
- Matrix: the value of ε_m control the position of the peak;
- Shape:
  - Spherical nanoparticles: Mie theory;
  - Ellipsoidal cluster: Gans theory; eccentricity can lead to the production of a double peak, or to birifrangent systems;
  - Core-shell shape: the two surfaces must be considered; theoretically, there is an invisibility condition, that can be pratically archived using metamaterials;

4.5 Interacting nanoparticles

Let f be the filling fraction of the system, i.e. the volume of the nanoparticles over the total volume:

$$f = \frac{N \cdot V}{V_{tot}} = \rho\frac{4}{3}\pi R^3$$

In the effective medium approximation, one can use the Maxwell Garnel approximation:

$$\frac{\varepsilon_{eff} - \varepsilon_m}{\varepsilon_{eff} + 2\varepsilon_m} = f\frac{\varepsilon - \varepsilon_m}{\varepsilon + \varepsilon_m}$$

If f is not negligible, the approximation is no more valid and the Bruggermann theory must be considered:

$$f\frac{\varepsilon - \varepsilon_{eff}}{\varepsilon + 2\varepsilon_{eff}} = (1-f)\frac{\varepsilon_m - \varepsilon_{eff}}{\varepsilon_m + 2\varepsilon_{eff}}$$

It's not hard to show that this is compatible with the Mie theory.

A particular attention shall be payed to the fact that f does not only affect the peak amplitude but also, if it is not negligible, the peak position. However, typically $f \lesssim 10\%$, and therefore the peak position dependence can be neglected.

4.5.1 Multimers

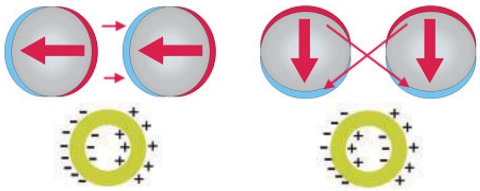

Figure 8: Couple of dipoles.

Consider a couple of dipoles, as in figure 8; depending on the polarization of the oscillation, the coupling of the dipoles can reduce (left) or increase (right) the resonance energy. A similar reasoning can be carried out for core-shell geometries, that can be considered as a couple of concentrical dipoles (sphere+cavity). The interaction between dipoles can be studied recalling hybridization schemes:

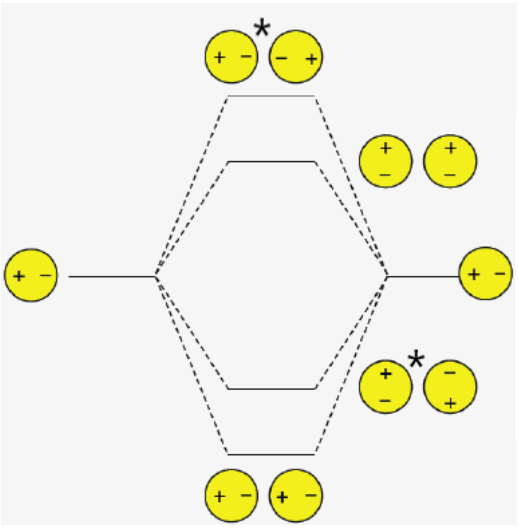

Figure 9: Dimers hybridization schemes. Note starred modes: they're called *dark plasmons*, because can't be excited from plane waves

Multi-particles extensions of Mie theory are available; moreover, in the gaps between nanoparticles, some hot points are created, where local field is really strongly enhanced. For example, in nanoplanets systems, between satellites and core very hot points are created.

Finally, long chains can affect peaks positions.

4.6 Discrete dipolar approximation DDA

To study a big object, one can consider it as made of lots of small dipoles. Consider, for example, N dipoles: when shining a plane wave $E = E_0 e^{i(kx-\omega t)}$ on the system, each dipole will react with a polarization

$$P_j = \alpha_j E_j$$

where the electric field perceived by each dipole is given by the external one plus all the other dipoles:

$$E_j = E_{ext,j} - \sum_{k \neq j} A_{jk} P_k$$

$$\implies \frac{P_j}{\alpha_j} + \sum_{k \neq j} A_{jk} P_k = E_{ext,j}$$

Considering the vectors $\tilde{P} = \{P_1, \dots, P_N\}$ and $\tilde{E}_{ext} = \{E_{ext,1}, \dots, E_{ext,N}\}$, one can define a matrix A and rewrite the last equation as

$$A\tilde{P} = \tilde{E}$$

i.e., to find the polarizations is enough to invert the matrix A. As the matrix is inverted, one can easily find the polarizations and the electric field all around the system.

4.7 Non linear responses

The polarization is only in first approximation linear with the electric field; some higher orders, in reality, are present:

$$P = \varepsilon_0(\chi^{(1)}E + \chi^{(2)}E^2 + \chi^{(3)}E^3 + \dots)$$

To study this higher orders, a strong incident field or hotspots properties can be used.

A notable effect due to $\chi^{(3)}$ is the Kerr effect: the dielectric function have a dependence from E^2, i.e. from the intensity: the dielectric function can be therefore tuned from outside the system itself, simply using different intensities!

$$\varepsilon = 1 + \frac{P}{\varepsilon_0 E} = 1 + \chi^{(1)} + \chi^{(3)}E^2$$

$$n = n_0 + n_2 I$$

$$\alpha = \alpha_0 + \beta I$$

with β that can be itself function of the intensity, and can also change sign!

4.8 Z-scan

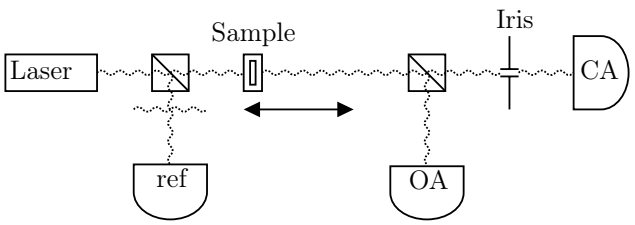

Figure 10: Z-Scan system

The system reported in fig. 10 permit to measure both n and α. In fact, the OA detector measure the intensity of the total laser beam, and can be used to study α; on the other hand, thanks to the iris the CA detector measure the intensity of the centre, and it's useful to study beam divergence and therefore n.

5 Observing nanoparticles

5.1 X-Ray diffraction

Remember the Bragg's law for diffraction from a periodic crystal: the maximums of diffractions are such that

$$k' - k = G$$

where k' and k are the incident and the scattered wave, while G is a vector in the reciprocal space. Being θ whe incident (and scattered) beam angle with respect to the crystal plane, the previous relation can be written as

$$2d \sin\theta = \lambda$$

where d is the distance between two subsequential planes,

$$d = \frac{a}{\sqrt{h_1^2 + h_2^2 + h_3^2}}$$

with (h_1, h_2, h_3) the plane Miller indices.

The exiting wave is therefore given by the transmitted one plus the scattering one:

$$\psi_{out} = \psi_0 \left[e^{ikx} + \mathrm{i} f(\theta) \frac{e^{ikz}}{r} \right]$$

with i given by the scattering phase shift, $f(\theta)$ being the structure factor and $1/r$ from the sphericity of the scattered wave. If the base unit is a polyatomic cell, one can write:

$$f(\theta) = \sum_j f_j(\theta) e^{iG \cdot r}$$

where the sum is over the basis atoms. Consider, for example, a monoatomic fcc structure: the basis atoms are in $(0,0,0)$, $(1/2, 1/2, 0)$, $(1/2, 0, 1/2)$ and $(0, 1/2, 1/2)$, and a plane with Miller indices (h,k,l). The structure factor is therefore:

$$\begin{aligned} f(\theta) &= f(G) \left[1 + e^{i\pi(h+k)} + e^{i\pi(h+l)} + e^{i\pi(k+l)} \right] \\ &= \begin{cases} 4f(G) & \text{if } h,k,l \text{ have all the same parity} \\ 0 & \text{otherwise} \end{cases} \end{aligned}$$

5.1.1 Peak broadening

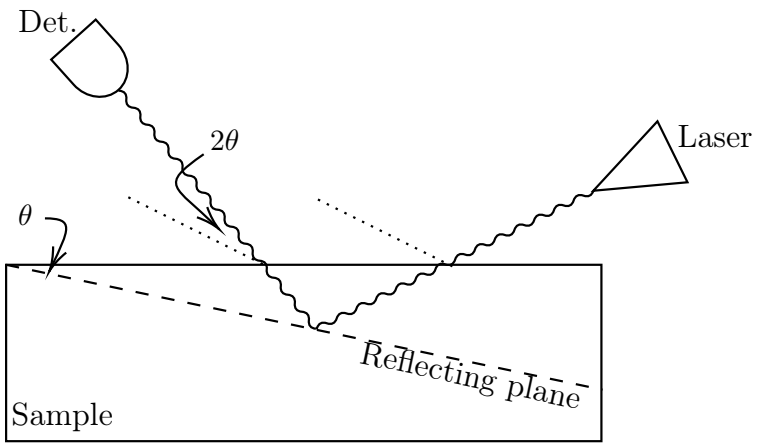

Figure 11: XRay measuring apparatus, with angles

The broadness of the reflection peaks can provide information of the properties of the nanoparticles. The total broadness of the peak is:

$$\beta_{obs} = \beta_{inst} \oplus \beta_{size} \oplus \beta_{strain} \oplus \dots$$

where $\oplus$ indicates a quadratic sum. Let's analyze all the appearing terms.

Instrumental The first term, β_{inst}, is the instrumental broadening given by the apparatus.

Size The second term is given by the nanoparticles size. The relation between the nanoparticle volume-weighted diameter D_v and the peak broadening is:

$$\beta_{size} = K\frac{\lambda}{D_v \cos\theta}$$

where K is the Scherrer constant, whose value depends on the definition of "broadness".

Strain The third term is present if the crystal is strained; given the average strain ε_{srt}, this component is:

$$\beta \propto \varepsilon_{srt} \tan\theta$$

... Some additive terms can results from other system characteristic, e.g. particles eccentricity.

5.2 Electron microscopy

An upper bound in microscopes resolution is given by the wavelength of the *particles* the microscope work with. Optical microscope, for example, works with photons: in the visible range, their wavelength is around 500nm, and therefore nanoparticles cannot be observed. To see at the nanoscale, one must switch to electron microscopes, which uses electrons with energy of keVs, i.e. wavelength in the order of picometers. Different types of electron microscope exists: e.g., the Transmission electron microscope TEM or the scanning one SEM. Both need a vacuum chamber to works, otherwise electrons will be scattered by air molecules. Most powerful TEM can reach sub-angstrom resolutions.

TEM observe transmitted electrons, and therefore need a thin layer of sample to properly work. On the other hand, SEM works with reflected ones, and can be used to study bulk materials. In a SEM, the electron source can be provided by thermo-ionic guns as well as by field emission guns.

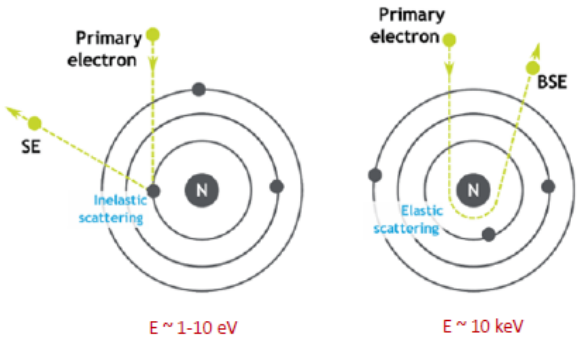

Figure 12: Main phenomena detected by SEM.

A SEM is provided of different detectors, which are able to detect different types of electrons. Secondary electrons (left in fig. 12) gives information about the tridimensional structure of the sample; backscattered electrons (right in 12), instead, can provide information about the composition of the sample. Finally, also XRay coming from atoms de-excitation can be measured, providing additive information on sample composition.

5.3 Near field optical properties

How the near-field optical properties can be studied?

5.3.1 Dark field optical microscopy

The idea is to measure only scattered light; with spectral analysis, one can study the shape of the nanoparticles. Sadly, to obtain a meaningful result, one must consider well-spaced nanoparticles, i.e. a low density system.

5.3.2 Electron energy loss spectroscopy

The idea here is to shot a fast (200keV) electrons beam, almost pointlike, which travel close to the particles. It induces excitations in the particles, and can excitate also dark plasmons (see fig. 9). The energy loss from the beam is:

$$\begin{aligned}\Delta E &= \int e\vec{v} \cdot \vec{E}_{ind}\,\mathrm{d}t \\ &= \int_0^\infty \Gamma(\omega)\,\mathrm{d}\omega\end{aligned}$$

with

$$\Gamma(\omega) = \frac{1}{\pi}\int \mathrm{d}t\,\Re(e\vec{v}\cdot\vec{E}_{ind}e^{-i\omega t})\,\mathrm{d}t$$

Studying $\Gamma(\omega)$, i.e. the energy absorption function, one can find plasmon resonances, both surface and bulk ones.

This spectroscopy can be used for studying size-dependent properties as well as for mapping near field properties.

6 Applications

6.1 Biosensing

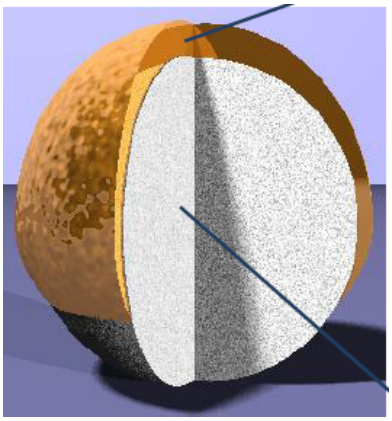

Figure 13: Dielectric core (polystyrene or silica) with a metallic half shell (Au,Ag, AuAg, Ni, Al, ...), typically in 2D array.

In biosensing, array of core-shell structure like the one in fig. 13 are frequently used. To produce them, the following method can be used:

- Nanosphere lithography: using a top-bottom technique, the basis is sculpted in a 2D array of dielectric nanospheres;
- Reactive ion etching: nanoparticles are reduces, leading to an array of smallest non-touching NPs;
- SNSA: gold is deposited from the top of the system.

The peculiarity of this system is to be very sensible to the stuff attached to the surface; is some bio-molecules attach to the gold shell, the optical peak moves and allow an estimation of composition and concentration of extraneous substances.

To permit to biological molecules to attach to the shell, it must be covered with receptors: consider, for example, a streptavidin biosensor: the gold shell is covered with biotin molecules, which act as receptors, and thiols, which are used to equally distribute biotin molecules. Remember that through ion etching one can control the size of the particles, and therefore the magnitude of the interaction. If the system is properly calibrated, one can find:

$$\Delta\lambda_{LPSR} = f([\text{streptavidin}])$$

6.2 Self-similar nanolens

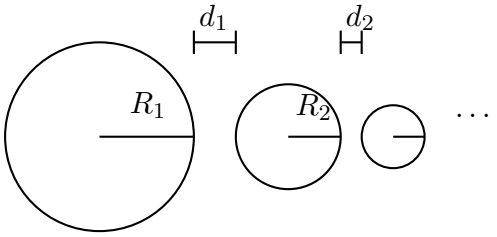

Figure 14: Nanolens structure

Consider a sequency of nanoparticles, of radius R_i and distance d_i, such that:

$$\begin{cases} R_{i+1} = sR_i \\ d_{i+1} = sd_i \end{cases} \qquad \text{with } s \ll 1$$

where the last condition allow each particle to be considered in the "near field" area of the bigger ones. This result in a large field enhancement:

$$E_n = f_e^n E_0$$

Typically, systems with $s = 0.3, N = 3$ are studied, as well as symmetric systems. Some of the applications of these systems are nanooptical detection, Raman characterization, nonlinear spectroscopy, nanomanipulation of single molecules or nanoparticles.

6.3 Emitters

Excited-state lifetime of emitters can be influenced by the proximity of a nanoparticle. Consider an emitter of dipolar radiation: the emission rate γ is the product of the excitation rate γ_{ex} and the quantum efficiency q_a. But:

- The quantum efficiency can be depressed by the levels of the nanoparticles, which contribute to the formation of more relaxation patterns;
- The excitation rate can be increased by near field enhancement.

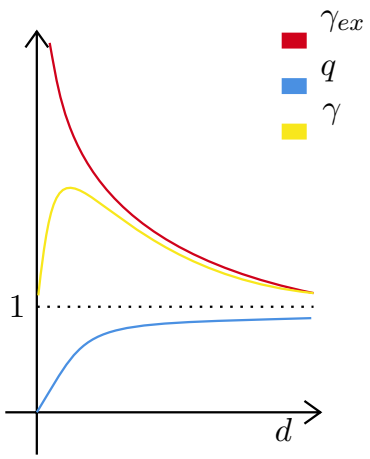

Figure 15: Quantum efficiency, excitation rate and emission rate, as function of the distance between the emitters and the nanoparticle.

The two effect combines (fig. 15) and results in a optimal distance between the nanoparticle and the emitters which maximize the emission rate.

Moreover, with array of nanoparticles surrounding the emitter, one can control the directionality of the emitted radiation.

7 Propagation and confinement of photons

In this sections, as well as in all this notes, we consider $\mu = 1$.

Remember that the dielectric function can be written as:

$$\varepsilon = (n + \mathrm{i}k)^2$$

where n is the refractive index and k the absorption coefficient. Remember the equations for electrons motion, and their solution in free space:

$$\left(-\frac{\hbar^2}{2m}\nabla^2 + V - i\hbar\frac{\partial}{\partial t}\right)\Psi = 0 \qquad \Psi = \Psi_0 e^{\mathrm{i}(kx-\omega t)} \qquad \omega = \frac{\hbar}{2m}k^2 + \frac{V}{\hbar}$$

and observe that they are similar to the photons ones:

$$\left(\nabla^2 - \frac{\varepsilon}{c^2}\frac{\partial^2}{\partial t^2}\right)E = 0 \qquad E = E_0 e^{\mathrm{i}(kx-\omega t)} \qquad \omega^2 = \frac{c^2}{\varepsilon}k^2$$

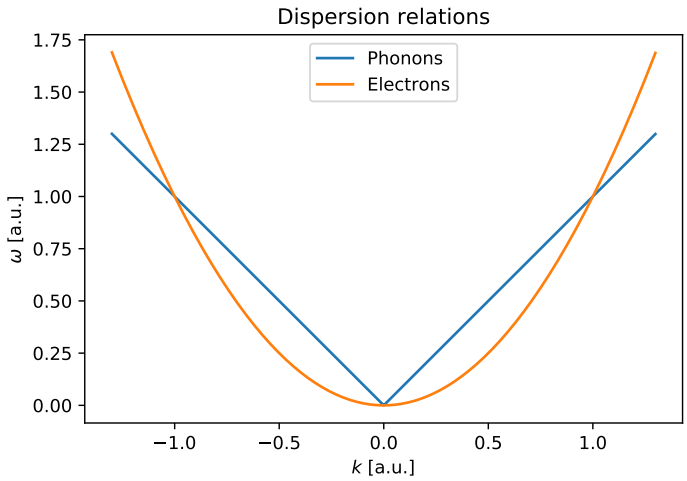

Figure 16: Dispersions relations

Observe that, in free space, phonon motion is not dispersive ($v_{ph} = v_g$) while electrons one is dispersive ($v_{ph} = 2v_g$).

Given the similarity of the two motions, one can archive phenomena typical of one particle with the other one; for example, the critical angle from snell Law: typically studied for photons, e.g. for transmitting signals in optical fibers, can be applied for electrons, confining them in potential wells! In this case, the potential V take for the electrons the same role that the refractive index n has for the phonons.

Moreover, consider a potential well, or a refractive index well (i.e., a zone with a low refractive index with respect to the surrounding one): the electrons are constrained in an harmonic motion inside the potential well and a exponential decay outside (skin effect) as well as the photons with the refractive index well. Tunneling effect, typical of electrons constrained by a thin barrier, can be observed even for phonons constrained by a thin high refractive index one.

One must point out that, while the potential is almost-freely tunable and high potential can be easily reached, for the refracting index it's a bit more complex and a not-so-wide refractive indices spectrum is available; however, effect like the ones cited before can be observed optimizing the barrier efficiency, e.g. exponential decay and tunneling can be observed when shining a beam against a not-so-high-refractive-index barrier with an angle greater than the critical one.

7.1 Photonic crystals

As well as typical crystal shows a periodic potential which affect the band structure of electron dispersion relation, there exists *photonic crystal*: they're structure with a periodic dielectric function, typically built using multilayers or nanoparticles arrays, to mimic electrons behavior in crystal with photons.

A structure similar to the band ones in electrons crystal can be obtained in photonic crystals! It's exactly as in the electronic central equation:

$$\varepsilon = \sum_G \varepsilon_G e^{iGr} \qquad E = \sum_k A_k e^{ikr}$$

$$\left(\nabla^2 + \varepsilon \frac{\omega^2}{c^2}\right) E = 0$$

Using the same procedure used for central equation*, one obtain, near to the intersection points, two solutions: a band gap open! The photons spectra is therefore no more continuous!

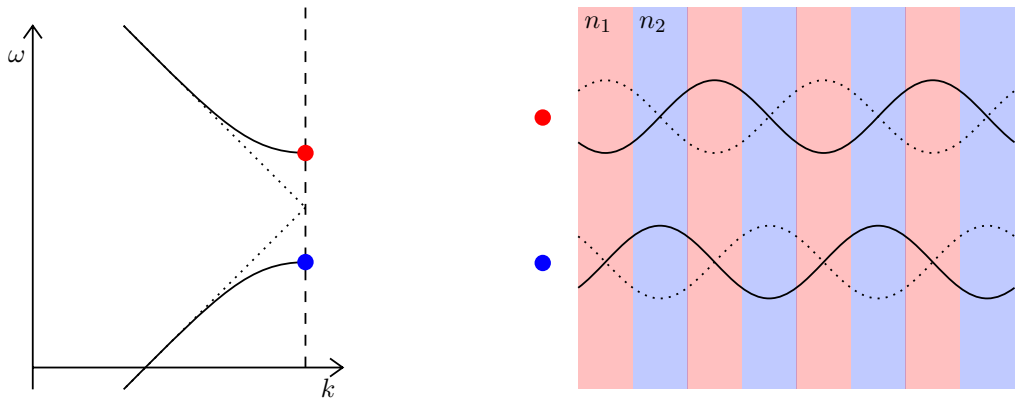

Figure 17: Band structure of phonons dispersion relation in a photonic crystal (left). Imagine the crystal made by a multilayer of alternating refractive number n_1 and n_2: observe that in the dispersion relation there are two stationary waves, i.e., with mull group velocity (red and blue marks). They correspond to the stationary waves with nodes in n_1 or in n_2 (right).

*Pay attention that in class the professor explain all the procedure, that is here not reported. Refer to solid state notes.

It's not hard to find, using perturbation theory, the width of the band gap:

$$\frac{\Delta\omega}{\omega} \approx \frac{\Delta\varepsilon}{\varepsilon}\frac{\sin \pi d/a}{\pi}$$

where d is the thickness of each layer.

Similar effects can be archived on polarization: lack of symmetries in some directions can lead to a disappearance of the degeneracy.

Over the periodicity, defect of the systems can be used to transmit waves. Defects, in fact, can provide states in the band gaps: using a proper wave, such that the transmission on the defects is possible while the transmission in the crystal is forbidden by band gap, one can direct the signal with a pathway of defects.

Multidimensional photonic crystalline structures also exists.

8 Metamaterials

Structure in which characteristic dimensions are comparable to optical wavelengths.

Positive and negative dielectric function

Remember that $\varepsilon = 1 + \chi_1 + \mathrm{i}\chi_2$.

- If ε is purely real, $\chi_2 = 0$: the medium is neither absorbing or enhancing the waves;
- In the presence of absorption, $\chi_2 < 0$, while $1 + \chi_1$ can be either positive or negative, and its positivity can be function of the wavelength;
- For an active media (such a laser), $\chi_2 > 0$.

As *metamaterials* is named a wide class of different thing, with the common characteristic of properly combining different existing materials to obtain structure with novel functionalities, e.g. particular optical properties.

Remembering that:

$$\left(n + \mathrm{i}\frac{\alpha}{2}\right)^2 = \varepsilon\mu$$

and considering non-dissipative ($\alpha = 0$) materials, there are clearly two possible situations: both ε and μ positive, or both negative. In nature, there are known cases of ε or μ negative, but never both.

A priori, there are also the "mixed" solutions, in which $\varepsilon\mu < 0$. In these cases, however, $n = 0$ and $\alpha \neq 0$: there are no propagation of the wave, but only absorption ($\lambda_{osc} \to \infty$, while λ_{dump} is finite and given by α). Finally, there are also the cases in which ε and/or μ are not real (refer to box at page 12)

The case of $\varepsilon, \mu < 0$ has been theoretically studied even before finding suitable materials. A particular effect regards the triplet $\vec{k}, \vec{E}, \vec{H}$: typically, this triplet is right-handed; in material with $\varepsilon, \mu < 0$, however, this triplet is left-handed! This means that the Poynting vector and the wavevector are in opposite direction, i.e. group velocity and phase velocity are opposite!

In a more formal way, one can define the matrix of direction cosines, and the parity coefficient:

$$p = \det(G) = \begin{cases} 1 & RH \\ -1 & LH \end{cases}$$

(the single-negative case, as stated before, is not considered since there is no wave propagation!)

Observe for example the effects on Snell law: remember the surface continuity constraints:

$$\begin{cases} E_{t1} = E_{t2} \\ \varepsilon_1 E_{n1} = \varepsilon_2 E_{n2} \end{cases}$$

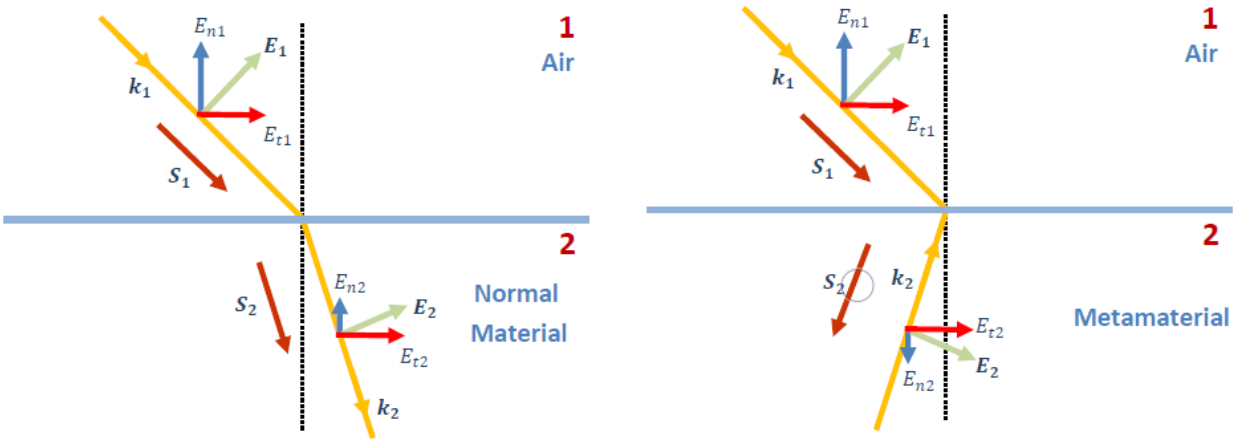

(a) Normal material: $\varepsilon > 0, \mu > 0$

(b) Metamaterial: $\varepsilon < 0, \mu < 0$

Figure 18: Snell law of rifraction

As can be seen in fig. 18, in the metamaterial the light beam change direction, and the wavevector is reversed! (but the Poynting vector goes in the right direction, keeping the energy conservation)

The Snell law therefore, considering the parity coefficients p_1 and p_2, becomes

$$\frac{\sin\theta_1}{\sin\theta_2} = \frac{p_2}{p_1}\left|\sqrt{\frac{\varepsilon_2\mu_2}{\varepsilon_1\mu_1}}\right|$$

which recast in the well-known Snell law if one define $n = p\sqrt{\mu\varepsilon}$, i.e. use negative refractive index for metamaterials.

Using metamaterials, lots of interesting and useful applications are possible; for example, perfect lenses, with spherical interfaces which null aberrations. Moreover, the known phenomena are inverted, like doppler effect.

8.1 Obtain metamaterials

To obtain a metamaterial, one must satisfy both $\varepsilon < 0$ and $\mu < 0$ conditions. The first one is easy to obtain: it's realized in lots of metals. On the other hand, $\mu < 0$ is hardest to archive: one must properly study system shape. Some existing techniques uses localized currents or magnetic resonances.

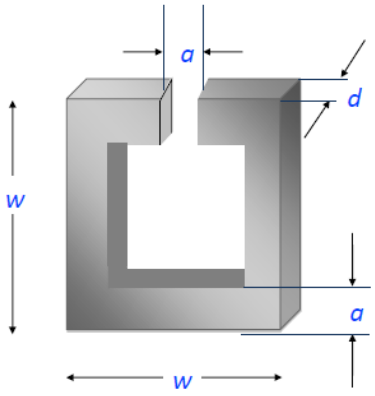

Figure 19: Split ring resonator

An example can be given by the split ring resonator: it works like a LC circuit, in which induced currents can lead, in some situations, to an negative apparent μ. An array of split ring resonator can be used in combination with metal bars, to allow the control of both ε and μ; this type of system can present frequency bands with ε and μ (almost) real and negative. However, the produced systems works at microwave frequencies; no optical frequencies working systems have been realized until today, since with the optical frequencies plasmonic effect appears.

8.2 Anisotropic metamaterials

Using periodical nanostructure, one can obtain anisotropic metamaterials. Consider for example a stack of two isotropic layers, with dielectric function ε_1 and ε_2 and filling fraction f and $1-f$. The effective field is given by the weighted mean of the fields in the two materials, and the dielectric function must be represented by a tensor:

$$\varepsilon = \begin{pmatrix} \varepsilon_{\parallel} & 0 & 0 \\ 0 & \varepsilon_{\parallel} & 0 \\ 0 & 0 & \varepsilon_{\perp} \end{pmatrix}$$

where it's not hard to show, using boundary continuity conditions, that

$$\varepsilon_{\parallel} = f\varepsilon_1 + (1-f)\varepsilon_2 \qquad \frac{1}{\varepsilon_{\perp}} = \frac{f}{\varepsilon_1} + \frac{1-f}{\varepsilon_2}$$

An opposite situation can be obtained with a 2D array of nanobars: in that case, there are two perpendicular directions and a parallel one, with:

$$\varepsilon_{\parallel} = f\varepsilon_1 + (1-f)\varepsilon_2 \qquad \varepsilon_{\perp} = \varepsilon_2 \frac{(1+f)\varepsilon_1 + (1-f)\varepsilon_2}{(1-f)\varepsilon_1 + (1+f)\varepsilon_2}$$

where typically $\varepsilon_{\parallel} < 0$!

8.3 Hyperbolic materials

Typical class of non-isotropic meta materials, in which the isocontours of k_0 in the k_x, k_y, k_z space are hyperbolic.

Remembering the equations for time-harmonic waves:

$$k \times H = -\omega D \qquad k \times E = \omega \mu_0 H$$

which results in

$$k \times k \times E = k \times \omega\mu_0 H = -\mu_0\omega^2 D = -\frac{\omega^2}{c^2}\varepsilon E$$
$$k \times k \times E = k(k \cdot E) - k^2 E \Rightarrow k(k \cdot E) - k_0^2 E + k_0 \varepsilon E = 0$$

where $k_0 = \frac{\omega^2}{c^2}$ and ε is a diagonal matrix. This lead to:

$$\begin{pmatrix} k_0\varepsilon_{xx} - k_y^2 - k_z^2 & k_x k_y & k_x k_z \\ k_x k_y & k_0\varepsilon_{yy} - k_x^2 - k_z^2 & k_y k_z \\ k_x k_z & k_y k_z & k_0\varepsilon_{zz} - k_x^2 - k_y^2 \end{pmatrix} E = 0$$

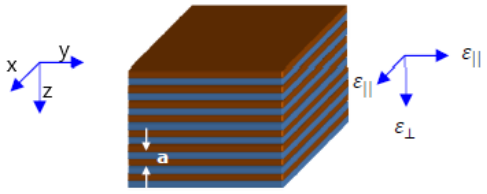

Figure 20: Multilayer materials

Solving the equation, i.e. imposing the matrix determinant at 0, considering a multilayer metamaterial like the one in fig. 20, one obtain two types of solutions:

- Ordinary waves: $E \perp z$, with the dispersion relation $k^2 = \varepsilon_{\parallel} k_0^2$

- Extraordinary waves: $\hat{E} \times \hat{x} = \cos\theta$, with the dispersion law

$$\frac{k_x^2 + k_y^2}{\varepsilon_\perp} + \frac{k_z^2}{\varepsilon_\parallel} = k_0^2$$

Remember that (Fresnel equations) waves intensity is dumped by k_0^2: but, if $\varepsilon_\parallel$ and $\varepsilon_\perp$ are discordant, k_0 can be small even with large k!

A material is called *hyperbolic* if $\varepsilon_\parallel \varepsilon_\perp < 0$. Hyperbolic materials can be classified in:

- Type I materials, if ε have only 1 positive entry;
- Type II materials, if ε have 2 positive entries.

The latter are particularly useful if coupled with emitters, since their density of states diverges.

Considering more complex structures, lots of different metamaterials can be obtained; playing with filling fractions, one can obtain a wide spectra of properties.

Finally, a notable class of materials are the *EpsilonNearZero* ones; in this materials, $n \to 0$: phase velocity and wavelength diverges, i.e. all photons in the material oscillates coherently. This result in an large enhancement of the optical gain.